Synthesis and Characterization of Sulfur-Ylide Complexes of Gold(I). Observance of Intermolecular Gold(I)−Gold(I) Interactions in Solution

Da-Fa Feng, Shaw Shiah Tang, C. W. Liu, and Ivan J. B. Lin*

Department of Chemistry, Fu-Jen Catholic University, Hsinchuang, Taipei 242, Taiwan

Yuh-Sheng Wen and Ling-Kang Liu*

Institute of Chemistry, Academia Sinica, Taipei 115, Taiwan

Received August 28, 1996[⊗]

Under PTC/OH^- (PTC = phase-transfer catalysis) conditions, the reaction of $Au_2(dppm)Cl_2$ (dppm = 1,1-bis(diphenylphosphino)methane) with $[Me_2S(O)NMe_2]BF_4$ produces a greenish luminescent compound $[Au_2(dppm)[(CH_2)_2S(O)NMe_2]]BF_4$, **1**, and a colorless tetranuclear compound $[Au_4(dppm)(Ph_2PCHPPh_2)[(\mu\text{-}CH)(CH_2)S(O)NMe_2]]BF_4$, **2**. Both compounds **1** and **2** also can be synthesized from $[Au_4(dppm)(Ph_2PCHPPh_2)Cl_3]$, **3**, which can be produced simply by the reaction of $Au_2(dppm)Cl_2$ with OH^- in the presence of a PTC. For $Au_2(dppe)Cl_2$ (dppe = 1,2-bis(diphenylphosphino)ethane) and $Au_2(dmpm)Cl_2$ (dmpm = 1,1-bis(dimethylphosphino)methane), only $[Au_2(dppe)[(CH_2)_2S(O)NMe_2]]PF_6$, **4**, and $[Au_2(dmpm)[(CH_2)_2S(O)NMe_2]]BF_4$, **5**, are obtained as the major product, respectively. Compounds **1**−**4** are characterized by single-crystal X-ray analyses. Two C_2-related cations of **1** are packed in a row with the intermolecular Au−Au distance (2.959 Å) shorter than the intramolecular Au−Au distance (2.984 Å). Compound **2** has one of the ylide carbon atoms bridging two gold(I) atoms. The tetragold cluster of **3** is formed by an Au−C linkage between $[ClAu(\mu\text{-}Ph_2PCH_2PPh_2)Au]^+$ and $[ClAu(\mu\text{-}Ph_2PCHPPh_2)AuCl]^-$. The digold cation of **4** is a nine-membered dimetallocycle. In acetonitrile solution, dimerization of **1** and **5** through intermolecular Au−Au interaction occurs as evidenced by concentration-dependent absorption spectroscopic studies. Concentration-dependent absorption spectra of **1** and **5** suggest that equilibriums between the monomer and dimer exist with equilibrium constants of 33 ± 9 and 52 ± 7 M^{-1} in acetonitrile, respectively. Digold(I) compounds **1**, **4**, and **5** luminesce in the solid state.

Introduction

One of the most intriguing characteristics of the metal−ylide complexes is that the rich coordination modes of ylides can provide a variety of structural information.[1] According to the latest review article[2] written by Kaska and Ostoja Starzewski, more than 13 different coordination modes have been observed in the phosphorus-ylide−metal complexes. For example, the ylidic carbon atom can act as a bridging atom to form homo- and/or heterometal clusters.[3] In contrast to the numerous examples known for the phosphorus-ylide−metal complexes,[1−4] examples of a similar bonding mode for the sulfur-ylide complexes are extremely rare.[5,14] The potential richness of sulfur-ylide compounds in bonding and the use of these compounds in organic[6] and organometallic reactions led us to this study.

Earlier we have used the phase-transfer catalysis (PTC) technique to synthesize sulfur-ylide complexes of palladium and platinum.[7] Lately we have extended the technique to the synthesis of gold compounds.[8] Not only is this technique is simple, but also the synthesis of sulfur-ylide complexes under PTC conditions may be relevant to the biosynthesis of presqualene pyrophosphate in water.[9] In our preliminary report,[8] we have

[⊗] Abstract published in *Advance ACS Abstracts,* February 1, 1997.

(1) (a) Johnson, A. W. *Ylides and Imines of Phosphorus*; J. Wiley & Sons: New York, 1993. (b) Kaska, W. C. *Coord. Chem. Rev.* **1983**, *48*, 1.

(2) (Kaska, W. C.; Ostoja Starzewski, K. A. In *Ylides and Imines of Phosphorus*; J. Wiley & Sons: New York, 1993; Chapter 14, p 485.

(3) (a) Churchill, M. R.; Young, W. J. *Inorg. Chem.* **1981**, *20*, 382. (b) Uedelhoven, W.; Neugebaure, D.; Kreissl, F. R. *J. Orgamet. Chem.* **1981**, *217*, 183. (c) Jeffery, J. C.; Navarro, R.; Razay, H.; Stone, F. G. A. *J. Chem. Soc., Dalton Trans.* **1981**, 2471. (d) Konig, H.; Menu, M. J.; Dartiguenave, M.; Dartiguenave, Y.; Klein, H. F. *J. Am. Chem. Soc.* **1990**, *112*, 5351. (e) Cramer, R. E.; Maynard, R. B.; Gilje, J. W. *J. Am. Chem. Soc.* **1978**, *100*, 5562.

(4) (a) Cerrada, E.; Gimeno, M. C.; Jimenez, J.; Laguna, A.; Laguna, M. *Organometallics* **1994**, *13*, 1470. (b) Bardaji, M.; Gimeno, M. C.; Jones, P. G.; Laguna, A.; Laguna, M. *Organometallics* **1994**, *13*, 3415. (c) Bardaji, M.; Jones, P. G.; Laguna, A.; Laguna, M. *Organometallics* **1995**, *14*, 1310.

(5) (a) Fackler, J. P., Jr.; Paparizos, C. *J. Am. Chem. Soc.* **1977**, *99*, 2363. (b) Stein, J.; Fackler, J. P., Jr.; Paparizos, C.; Chen, H.-W. *J. Am. Chem. Soc.* **1981**, *103*, 2192. (c) Yamamoto, Y. *Bull. Chem. Soc. Jpn.* **1987**, *60*, 1189. (d) Konno, H.; Yamamoto, Y. *Bull. Chem. Soc. Jpn.* **1987**, *60*, 2561.

(6) (a) Corey, E. J.; Chaykovsky, M. *J. Am. Chem. Soc.* **1965**, *87*, 1353. (b) Trost, B. M.; Melvin, L. S. *Sulfur Ylide*; Academic Press: New York, 1966.

(7) (a) Lin, I. J. B.; Lai, H. Y. C.; Wu, S. C. *J. Organomet. Chem.* **1986**, *309*, 225. (b) Wu, R. F.; Lin, I. J. B.; Lee, G. H.; Cheng, M. C.; Wang, Y. *Organometallics* **1990**, *9*, 126. (c) Lai, J. S.; Wu, R. F.; Lin, I. J. B.; Cheng, M. C.; Wang, Y. *J. Organomet. Chem.* **1990**, *393*, 433.

(8) Lin, I. J. B.; Liu, C. W.; Liu, L.-K.; Wen, Y.-S. *Organometallics* **1992**, *11*, 1447.

(9) Cohen, T.; Herman, G.; Chapman, T. M.; Kuhn, D. *J. Am. Chem. Soc.* **1974**, *96*, 5627.

S0276-7333(96)00748-0 CCC: $14.00

Scheme 1

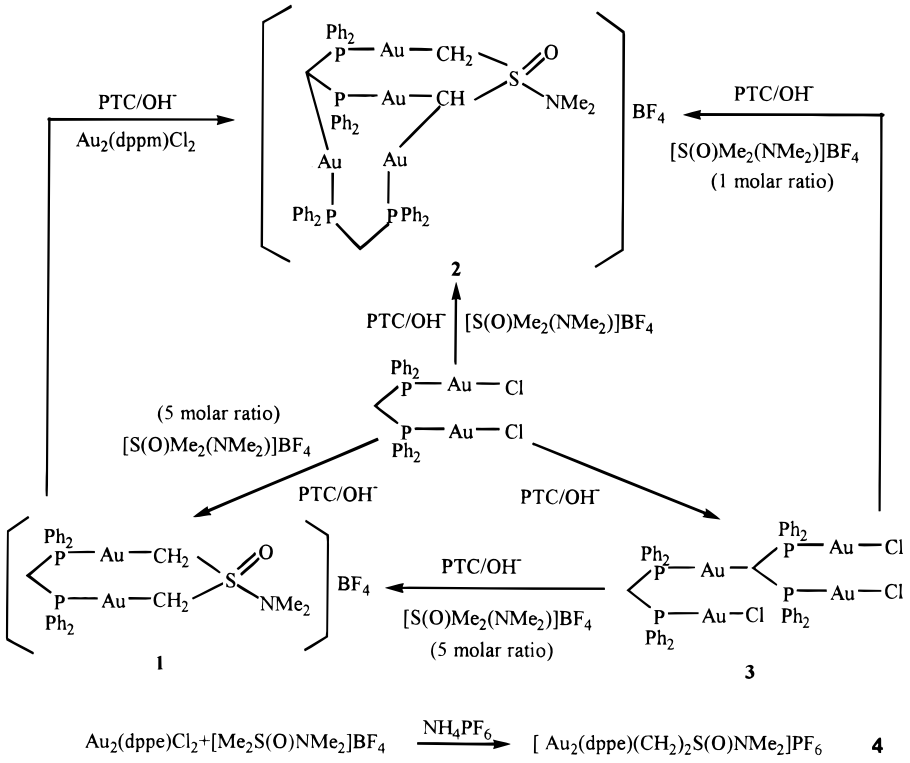

$$Au_2(dppe)Cl_2 + [Me_2S(O)NMe_2]BF_4 \xrightarrow{NH_4PF_6} [Au_2(dppe)(CH_2)_2S(O)NMe_2]PF_6 \quad \mathbf{4}$$

demonstrated that the PTC technique enables us to synthesize an annular eight-membered digold(I) sulfur-ylide complex and a tetranuclear gold(I) sulfur-ylide complex. The former dimerizes in the solid state with the intermolecular Au−Au distance shorter than the intramolecular Au−Au distance, and the latter has one of the ylidic carbon atoms bridging two Au(I) atoms.

Recently, the influence of Au−Au interactions on the photophysical and -chemical properties of gold(I) compounds has received much attention.[10] Annular gold(I) complexes, which are eight-membered rings, have been of special interest because the constrained Au−Au interactions may enhance photoluminescence.[11] The digold(I) sulfur-ylide complex **1** reported in this work indeed shows a bright green luminescence in the solid under daylight. The bright green emission in the solid state is probably due to the linear Au_4 unit. It would be of interest to compare the nature of Au−Au interactions with that in the eight-membered and that in the nine-membered annular digold(I) compounds.

Here we report the details of the synthesis and characterization of the eight- and nine-membered digold(I) complexes of sulfur ylides together with two tetranuclear Au(I) compounds. The photoluminescent properties of digold(I) complexes are included. Interestingly, we are able to show that molecular association of eight-membered annular digold(I) compounds occurs in solution.

(10) (a) Assefa, Z.; McBurnett, B. G.; Staples, R. J.; Fackler, J. P., Jr.; Assmann, B.; Angermaier, A. K.; Schmidbaur, H. *Inorg. Chem.* **1995**, *34*, 75. (b) Shieh, S. J.; Hong, X.; Peng, S. M.; Che, C. M. *J. Chem. Soc., Dalton Trans.* **1994**, 3067. (c) Yam, V. W. W.; Choi, S. W. K. *J. Chem. Soc., Dalton Trans.* **1994**, 2057. (d) Yam, V. W. W.; Lee, W. K. *J. Chem. Soc., Dalton Trans.* **1993**, 2097. (e) Yam, V. W. W.; Lai, T. F.; Che, C. M. *J. Chem. Soc., Dalton Trans.* **1990**, 3747. (f) Che, C. M.; Kwong, H. L.; Yam, V. W. W.; Poon, C. K. *J. Chem. Soc., Dalton Trans.* **1990**, 3215.

(11) (a) King, C.; Wang, J. C.; Khan, Md. N. I.; Fackler, J. P., Jr. *Inorg. Chem.* **1989**, *28*, 2145. (b) Che, C. M.; Kwong, H. L.; Yam, V. W. W.; Cho, K. C. *J. Chem. Soc., Chem. Commun.* **1989**, 885.

Results and Discussion

Synthesis. Under various PTC/OH^- conditions, reaction of $Au_2(dppm)Cl_2$ (dppm = 1,1-bis(diphenylphosphino)methane) with $[Me_2S(O)NMe_2]BF_4$ produced a greenish luminescent compound $[Au_2(dppm)[(CH_2)_2S(O)NMe_2]]BF_4$, **1**, a colorless tetranuclear compound $[Au_4(dppm)(Ph_2PCHPPh_2)[(\mu\text{-}CH)(CH_2)S(O)NMe_2]]BF_4$, **2**, and another colorless tetranuclear compound $[Au_4(dppm)(Ph_2PCHPPh_2)Cl_3]$, **3** (see Scheme 1). Formation of compound **1** was favored by the reaction of $Au_2(dppm)Cl_2$ with a 5-fold excess of sulfoxonium salt and NaOH. Compound **2** was the favorable product when the base was increased to a 100-fold excess. When the molar ratios of sulfoxonium salt, NaOH, and $Au_2(dppm)Cl_2$ were 1.0:0.5:1.0, the major product was compound **3**. Compound **3** could also be produced by the reaction of $Au_2(dppm)Cl_2$ with OH^- in the presence of a PTC. When $Au_2(dppe)Cl_2$ (dppe = 1,2-bis(diphenylphosphino)ethane) instead of $Au_2(dppm)Cl_2$ was reacted with $[Me_2S(O)NMe_2]BF_4$ under PTC/OH^- conditions, only $[Au_2(dppe)[(CH_2)_2S(O)NMe_2]]PF_6$, **4**, was obtained as the major product after treatment with NH_4PF_6 (see Scheme 1).

It appears that compounds **1**, **4**, and **5** are formed from the direct reaction of $Au_2[R_2P(CH_2)_nR_2]Cl_2$ (R = Ph, Me; $n = 1$ or 2) with sulfur ylides. Under PTC/OH^- conditions, deprotonation of the $[Me_2S(O)NMe_2]^+$ in the aqueous phase produces sulfur ylides. The ylide will then diffuse into the organic layer to react with $Au_2(dppm)Cl_2$, $Au_2(dppe)Cl_2$, or $Au_2(dmpm)Cl_2$ (dmpm = 1,1-bis(dimethylphosphino)methane). The monodentate Au(I) ylide intermediates undergo transylidation to produce **1**, **4**, and **5**. This type of reaction has been successfully demonstrated in our previous work,[7] where the sulfur ylide normally acts as a monodentate or a chelating ligand in palladium(II) and platinum(II) complexes. Here the sulfur ylide acts as a bidentate

bridging ligand. Attempts to isolate the monodentate Au(I) ylide intermediates by methods other than the PTC technique have not been successful to date. In fact this type of complex has been reported only on two occasions.[5c,12] The monodentate Au(III) sulfur-ylide complex has been structurally characterized by Fackler *et al.*[5a,b]

Normally we used the trimethyloxosulfonium salt as a sulfur-ylide precursor in the synthesis of palladium(II) and platinum(II) complexes under PTC conditions.[7] However we did not succeed in the formation of Au(I) sulfur-ylide compounds using the same ylide precursor. Fortunately, the N,N′-dimethyl-substituted dimethylsulfoximine salt gave satisfactory results. Schmidbaur *et al.* pioneeringly used the sulfoximine salt as a sulfur-ylide precursor to react with main group elements,[13] the reaction being carried out under drastically anaerobic conditions. Weber also reported a similar reaction in the formation of a chromium compound.[14] Several Pd(II) and Pt(II) sulfur-ylide complexes with the same type of ylide also have been isolated under PTC conditions. The details will be reported in elsewhere. It is interesting to note that Vicente *et al.* successfully synthesized Au(I) sulfur-ylide complexes from the reaction of $[Me_3S(O)]ClO_4$ with Au(acac)PPh_3 (acac = acetylacetonato) in acetone at room temperature.[12]

Compound **3** is formed by the deprotonation of a bridging dppm methylene proton of the $Au_2(dppm)Cl_2$ to give $[Au_2(Ph_2PCHPPh_2)Cl_2]^-$ followed by the reaction of the anion with a second molecule of $Au_2(dppm)Cl_2$. Deprotonation of a methylene proton on the coordinated dppm molecule is facile.[15] Further coordinating the deprotonated dppm ligand to various metal ions including the Au(I) ion has been reported.[15] It is conceivable that the isolobal relationship between the proton unit and L−Au(I) unit (L = a general tertiary phosphine) makes the reaction facile.[16]

One may imagine that **2** can be produced by the consecutive deprotonations of a dppm methylene proton and an ylidic methylene proton from **1** and the stepwise reactions with $Au_2(dppm)Cl_2$. Therefore formation of **2** is favored by the high concentration of base. When **1** is reacted with OH^- in the presence of $Au_2(dppm)Cl_2$, it indeed produces **2**, although in poor yield. Alternatively, one may also imagine that **2** can be produced by the reaction of **3** with sulfur ylide to form a monodentate Au(I) ylide intermediate, followed by successive transylidation and deprotonation of a ylidic methylene proton. When **3** is reacted with sulfoxonium salt in a 1:1 molar ratio under similar PTC/OH^- conditions, **2** is produced in a 50% yield. However, when **3** is reacted with sulfoxonium salt in a 1:5 molar ratio under PTC/OH^- conditions, **1** instead of **2** results in a 80% yield. Thus, the amount of sulfoxonium salt controls the formation of **1** or **2** from **3**. In the formation of **1** from **3**, the Au−C bond in **3** is cleaved in the presence of sulfur ylide. That the deprotonation of a ylidic methylene proton producing an ylidic anion which coordinates to another metal atom is unknown for metal sulfur-ylide complexes prior to this work. Only recently has the formation of a hypercoordinate ylidic carbon atom from the stepwise deprotonation of ylidic methylene protons with acac followed by metalation with $Au(PPh_3)^+$ units been communicated.[12] The remarkable ease of formation of multinuclear gold compounds has been attributed to the auriophilicity.[17]

Formation of **3** from $Au_2(dppm)Cl_2$ under PTC/OH^- conditions is believed to be a major reaction; further reaction of **3** with sulfur ylide yields **1** and **2**. Another major reaction is likely the direct reaction of $Au_2(dppm)Cl_2$ with sulfur ylide to produce **1**. This reaction is also the only major reaction in the reaction of sulfur ylide with $Au_2(dppe)Cl_2$ in which dppe can not be deprotonated under PTC/OH^- conditions. Although **2** can be produced either from **1** or **3**, the simple product obtained from **3** and the complicated products obtained from **1** suggest that the most likely route of formation of **2** is through **3**.

All dinuclear Au(I) compounds **1**, **4**, and **5** show a simple singlet in the ^{31}P NMR spectra. The chemical shifts are at 36.44, 35.79, and 15.97 ppm, respectively. The tetranuclear compound **2** shows an ABCD pattern in the ^{31}P NMR spectrum. Two doublets centered at 36.44 ppm and 36.33 ppm, both having coupling constants of 14 Hz, can be reasonably assigned as the chemical shifts of the triply bridging dppm P atoms. The resonance of the P atom trans to the methine carbon atom is at 32.87 ppm which is a doublet of triplets. Another doublet centered at 28.00 ppm ($^2J_{PP}$ = 52 Hz) is the resonance of the remaining P atom. The ^{31}P NMR spectrum of compound **3** shows a typical AA′BC pattern. The resonance of the two chemically equivalent phosphorus nuclei of the triply bridging dppm ligand is at 30.36 ppm. The coupling constant between these two P atoms and the third P atom trans to the methine carbon atom is 15 Hz. A doublet of triplets at 35.53 ppm ($^2J_{PP}$ = 63 Hz, $^3J_{PP}$ = 15 Hz) is observed for the third P atom. A doublet centered at 24.73 ppm ($^2J_{PP}$ = 63 Hz) is the resonance of the fourth P atom. All the complexes but **3** show complicated ^1H NMR spectra. Compound **1** has a ABX_2 pattern for the dppm methylene protons and a AA′BB′XX′ pattern for the ylidic methylene protons. The latter pattern for the ylidic methylene protons also is observed in compounds **4** and **5**. In the ^1H NMR spectrum of **3** the resonance due to the CH proton appears as a triplet of doublets at 4.59 ppm ($^2J_{PH}$ = 12 Hz, $^3J_{PH}$ = 7 Hz) while a triplet centered at 3.35 ppm corresponds to the resonance of the dppm methylene protons.

Structures. The crystal structure of **1** consists of discrete digold cations and BF_4^- anions. Shown in Figure 1 is an ORTEP presentation of the digold cation dimer with selected bond angles and bond distances given in the figure caption. The cation is an eight-membered dimetallocycle with two Au atoms being doubly bridged with a $(CH_2)_2S(O)NMe_2^-$ ligand and a dppm ligand, the P−Au−C fragments being linear. The

(12) Vicente, J.; Chicote, M. T.; Guerrero, R.; Jones, P. G. *J. Am. Chem. Soc.* **1996**, *118*, 699.
(13) Schmidbaur, H.; Kammel, G. *Chem. Ber.* **1971**, *104*, 3252.
(14) Weber, L. *Angew. Chem., Int. Ed. Engl.* **1983**, *22*, 516.
(15) (a) Uson, R.; Laguna, A.; Laguna, M.; Manzano, B. R.; Jones, P. G.; Sheldrick, G. M. *J. Chem. Soc., Dalton Trans.* **1984**, 839. (b) Uson, R.; Laguna, A.; Laguna, M.; Manzano, B. R.; Jones, P. G.; Fittschen, C.; Sheldrick, G. M. *J. Chem. Soc., Chem. Commun.* **1986**, 509. (c) Van der Velden, J. W. A.; Bour, J. J.; Vollenbrock, B. P. T.; Smiths, J. M. M. *J. Chem. Soc., Chem. Commun.* **1979**, 1162. (d) Uson, R.; Laguna, A.; Laguna, M.; Lazaro, I.; Jones, P. G. *Organometallics* **1987**, *6*, 2326. (e) Falvello, L. R.; Fornies, J.; Navarro, R.; Reuda, A.; Urriolabeitia, E. P. *Organometallics* **1996**, *15*, 309.
(16) (a) Lauher, J. W.; Wald, K. J. *J. Am. Chem. Soc.* **1981**, *103*, 7648. (b) Hoffmann, R. *Angew. Chem., Int. Ed. Engl.* **1982**, *21*, 711.
(17) (a) Jones, P. G. *Gold Bull.* **1981**, *14*, 1021; **1986**, *19*, 46. (b) Schmidbaur, H. *Gold Bull.* **1990**, *23*, 11.

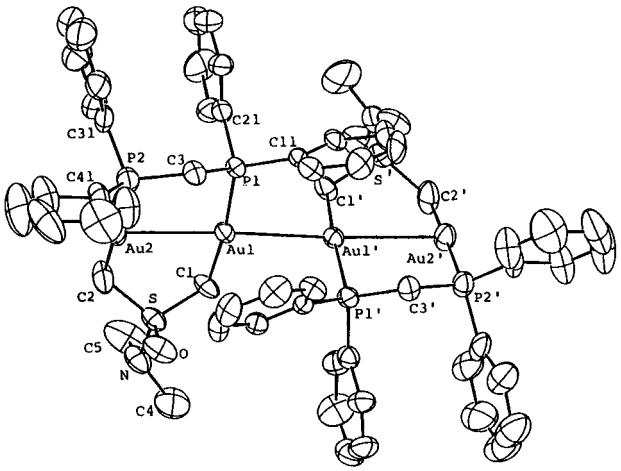

Figure 1. ORTEP plot of the dimeric structure of digold complex **1**. Selected bonded distances (Å): Au1−P1 2.289(3), Au−C1 2.088(12), Au2−P2 2.274(4), Au2−C2 2.097(14), Au1--Au1′ 2.959(1), Au1--Au2 2.984(1). Selected bond angles (deg): P1−Au1−C1 172.8(4), P2−Au2−C2 176.7(4). Selected torsional angles (deg): P1−Au1--Au2−P2 −11.1(1), P1−Au1--Au2−C2 165.7(4), C1−Au1--Au2−P2 174.4(3), C1−Au1--Au2−C2 −8.9(5), P1−Au1--Au1′−P1′ 94.5(1), P1−Au1--Au1′−C1′ −90.6(3), C1−Au1--Au1′−C1′ 84.3(4).

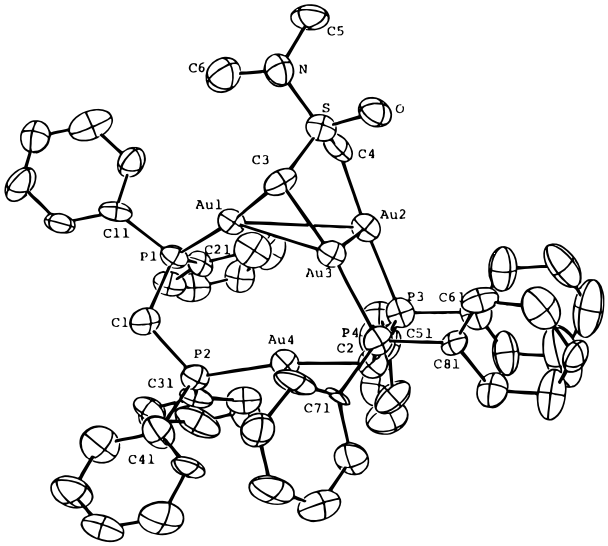

Figure 2. ORTEP plot of the tetragold cluster cation of **2**. Selected bond lengths (Å) and angles (deg): Au1−P1 2.264(7), Au1−C3 2.05(3), Au2−P3 2.305(8), Au2−C4 2.11(3), Au3−P4 2.293(7), Au3−C3 2.08(2), Au4−P2 2.295(7), Au4−C2 2.15(3), Au1--Au2 3.394(2), Au1--Au3 3.035(2), Au1--Au4 3.711(2), Au2--Au3 2.993(2), Au2--Au4 3.922(2), Au3--Au4 3.635(2); P1−Au1−C3 174.2(7), P3−Au2−C5 176.6(8), P4−Au3−C3 167.5(7), P2−Au4−C2 170.2(8), Au1−C3−Au3 94.4(10).

eight-membered ring is in a boat conformation with the S atom and methylene C atom of dppm as the head and tail. The most interesting features of the structure are that two C_2-related cations are packed together such that four Au atoms are in a row, with the intermolecular Au1−Au1′ distance (2.959 Å) shorter than the intramolecular Au1−Au2 distance (2.984 Å), and the six-atom plane (Au1, Au2, P1, P2, C1, and C2) in one cation is perpendicular to the corresponding plane in C_2-related cation. Compound **4** with a PF_6^- anion instead of BF_4^- has also been structurally characterized by X-ray diffraction. A similar digold cation dimer has also been found with the intermolecular Au−Au distance being shorter than the intramolecular Au−Au distance (2.913 Å vs 2.956 Å).[18]

The crystal structure of compound **2**, as determined by X-ray crystallography, includes discrete tetragold cluster cations, BF_4^- anions, and H_2O molecules. Shown in Figure 2 is the ORTEP plot of a tetragold cluster cation with selected bond angles and bond distances given in the figure caption. A deprotonated dppm ligand bridges three Au atoms (Au2, Au3, and Au4) through two P atoms and one methylene C atom, and a sulfur-ylide dianion also bridged three Au atoms through ylidic carbon atoms C3 and C4 (C3 bonded to both Au1 and Au3 and C4 to Au2). The arrangement is a triangular geometry (Au1, Au2, and Au3) with Au−Au contacts at 2.993, 3.035, and 3.394 Å. The fourth gold atom (Au4) is positioned at much longer Au−Au contacts with the above three (>3.635 Å). Bridging triangular Au complexes have been known in which the Au−Au distances are normally in the range of 3.2−3.4 Å.[19] If one disregards the Au−Au contacts, each Au atom seems to connect one C atom and one P atom, with P−Au−C angles ranging from 167.5(7) to 176.6(8)°. A highly strained ylidic C3 is revealed [angle Au1−C3−Au3 = 94.4(10)°]. It is noticeable that the bond distances between the S and two ylidic carbon atoms are different. S−C3, 1.69(3) Å, is shorter than S−C4, 1.75(3) Å.

The crystal structure of compound **3** consists of neutral tetragold clusters and CH_3CH_2OH molecules in a 1:1 ratio. The ORTEP plot of compound **3** in Figure 3 clearly shows that the tetragold cluster is formed by an Au−C linkage between $[ClAu(\mu\text{-}Ph_2PCH_2PPh_2)Au]^+$ and $[ClAu(\mu\text{-}Ph_2PCHPPh_2)AuCl]^-$. Selected bond angles and bond distances are given in the figure caption. The structural parameters in the Au−PCH_2P−Au portion of the former conform closely to the reported values (vide infra), e.g., torsional angle P1−Au1--Au2−P2 of 11.1(1)° with Au−Au distance of 3.188(1) Å; those in the Au−PCHP−Au portion of the latter exhibit noted deviations toward higher values—26.4(1)° and 3.247(1) Å—in a corresponding order, presumably due to a strain in joining an Au atom to the original methylene C atom of dppm. There is a substantial trans influence in Au3−P3 (2.277(5) Å, which is trans to the carbon atom) in comparison with the remaining Au−P distances (averaged 2.233(5) Å, trans to the chloride atom).

The crystal structure of compound **4** consists of discrete monomeric digold cations, PF_6^- anions, and two CH_2Cl_2 molecules. One of the CH_2Cl_2 molecules is disordered with more than one orientation in the solid state. Two types of PF_6^- anions exist in the structure: one is located on a crystallographic center and the other is on a general position with half the occupancy. Revealed in Figure 4, the digold cation exhibits a nine-membered dimetallocycle with two Au centers doubly bridged by a $(CH_2)_2S(O)NMe_2^-$ ligand and a dppe ligand. Selected bond angles and bond distances are given in the figure caption. Both P−Au−C fragments are approximately linear—173.2(1) and 174.9(1)° bond angles. The Au−Au distance, 3.119(2) Å, is much longer than that in **1**, 2.984 Å. The shortest intermolecular Au−

(18) Lin, I. J. B.; Liu, L. K. Unpublished result.
(19) (a) Minghetti, G.; Bonati, F. *Inorg. Chem.* **1974**, *13*, 1600. (b) Tiripicchio-Camellini, M.; Minghtti, G. *J. Organomet. Chem.* **1979**, *171*, 399. (c) Murray, H. H.; Raptis, R. G.; Fackler, J. P., Jr. *Inorg. Chem.* **1988**, *27*, 26. (d) Raptis, R. G.; Fackler, J. P., Jr. *Inorg. Chem.* **1990**, *29*, 5003.

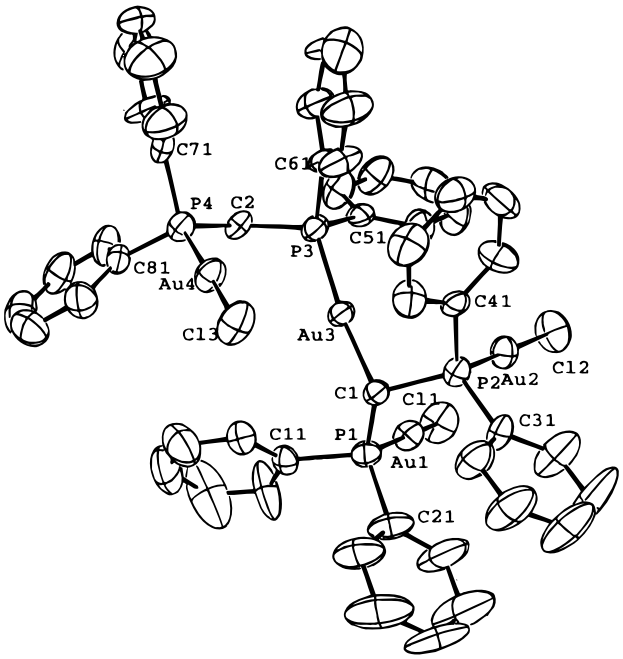

Figure 3. ORTEP plot of compound **3**. Selected bonded lengths (Å): Au1--Au2 3.188(1), Au1−P1 2.235(5), Au1−Cl1 2.289(5), Au2−P2 2.234(5), Au2−Cl2 2.279(5), Au3--Au4 3.2474(14), Au3−P3 2.277(5), Au3−C1 2.122(17), Au4−P4 2.230(5), Au4−Cl3 2.268(5). Selected bond angles (deg): P1−Au1−Cl1 173.2(2), P2−Au2−Cl2 176.7(2), P3−Au3−C1 173.8(5), P4−Au4−Cl3 175.2(2). Selected torsion angles (deg): P1−Au1--Au2−P2 −1.1(1), P1−Au1--Au2−Cl2 178.1(2), Cl1−Au1--Au2−P2 177.2(1), Cl1−Au1--Au2−Cl2 −3.6(2), P2−Au3--Au4−P4 169.8(1), P2−Au3--Au4−Cl3 −8.5(1), P3−Au3--Au4−P4 26.4(1), P3−Au3--Au4−Cl3 −152.0(1), Cl−Au3--Au4−P4 −157.7(3), Cl−Au3--Au4−Cl3 24.0(3).

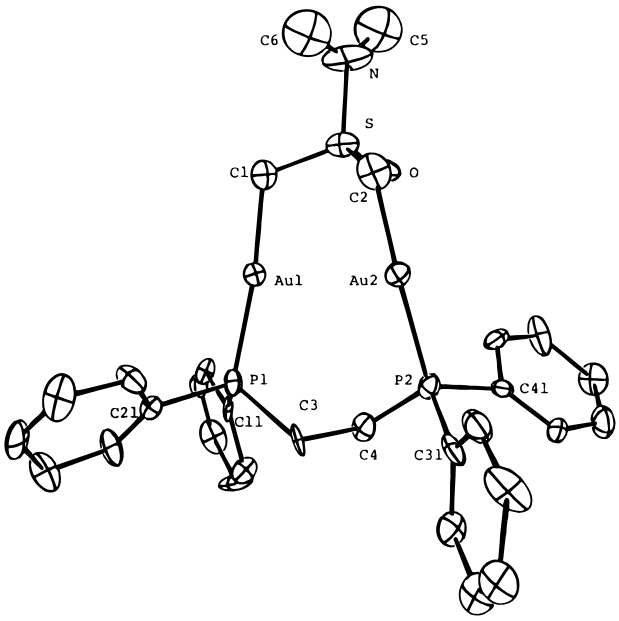

Figure 4. ORTEP plot of the digold cation of **4**. Selected bond distances (Å): Au1--Au2 3.119(2), Au1−P1 2.250(11), Au1−C1 2.04(4), Au2−P2 2.248(10), Au2−C2 2.00(4), S−C1 1.71(4), S−C2 1.69(4). Selected bond angles (deg): P1−Au1−C1 173.2(11), P2−Au2−C2 174.9(10), O−S−N 104.1(19), O−S−C1 116.9(21), O−S−C2 108.5(19), N−S−C1 114.1(21), N−S−C2 113.9(23), C1−S C2 99.6(22). Selected torsion angles (deg): P1−Au1--Au2−P2 20.7(3), P1−Au1--Au2−C2 −164.5(11), C1−Au1--Au2−P2 −164.8(12), C1−Au1--Au2−C2 10.0(16), O−S−N−C5 2.1(47), O−S−N−C6 −178.8(46), P1−C3−C4−P2 −108.0(23)°.

Au distance is 5.696(3) Å. Yet the torsional angle of P−Au--Au−P in **4** is 20.7(3)°, much larger than the corresponding angle of 11.1(1)° in **1**. The torsional angle of P1−C3−C4−P2 is 108.0(2)°, C3 and C4 being on different sides of the Au_2P_2 plane. The nature of the $(CH_2)_2S(O)NMe_2^-$ ligand in **4** is found to have a planar N atom, the sum of surrounding angles around N being 359°. Furthermore the pπ−dπ−pπ interactions of the N, S, and O atoms are strong, as evidenced by the coplanarity of the S=O vector and the SNC_2 skeleton; the torsional angles O−S−N−C5 and O−S−N−C6 are 2.1(5) and 178.8(5)°, respectively. On the contrary, the N atom of the $(CH_2)_2S(O)NMe_2^-$ ligand in **1** is clearly pyramidal: the sum of angles around N is 340.9° with torsional angle O−S−N−C5 = 177.6° and O−S−N−C6 = −51.1°. The N atom of the $(CH_2)_2S(O)NMe_2^-$ ligand in **2** is also pyramidal: the sum of angles around N is 345.0° with two corresponding torsional angles of −176.2 and 47.4°. The bonding geometry of the S atom in **4** is distorted from a tetrahedron, i.e., C1−S−C2 = 99.6(2)°. The corresponding angles are 107.5(7) and 106.3(1)° in **1** and **2**, respectively.

Several structural features observed in compound **1** need to be further discussed. First, the boat conformation of the eight-membered ring is unique in the dimetallocycle Au(I) chemistry. Most of the complexes, e.g. $[Au(CH_2)_2PR_2]_2$ (R = alkyl, Ph),[20] $[Au_2(dppm)_2]^{2+}$,[21] and $[Au(S_2P(OC_3H_7)_2)]_2$,[22] etc., have a chair conformation. Second, a chainlike molecule with Au(I) eight-membered dimetallocycles normally exhibits a shorter intermolecular than intramolecular Au−Au distance. In sharp contrast, compound **1** is a discrete digold(I) dimer in the solid state. The best description of **1** may be a tetranuclear Au(I) dication in which two dimetallocycles are linked together by the strong Au−Au interaction. Third, compound **1** is a discrete Au(I) molecule having four gold atoms in a row. The structures of gold complexes having four gold atoms in a row have been reported.[23] A pentanuclear gold complex that has a linear chain of gold atoms in different oxidation states, $[Au(II)]_2-Au(I)-[Au(II)]_2$, has been reported by Uson *et al.*[24]

The Au−Au interaction in **4** is regarded to be a relatively weak one, and that in **1**, a strong one. Attractive Au−Au interactions of ca. 3 Å are often compared in strength to a typical hydrogen bond (7−8 kcal/mol),[25] and the parallel has been made between the

(20) Schmidbaur, H.; Mandl, J. E.; Richter, W.; Bejenke, V.; Franke, A.; Huttner, G. *Chem. Ber.* **1977**, *110*, 2236.

(21) Schmidbaur, H.; Wohlleben, A.; Schubert, U.; Frank, A.; Huttner, G. *Chem. Ber.* **1977**, *110*, 2751.

(22) Lawton, S. L.; Rohrbaugh, W. J.; Kokotailo, G. T. *Inorg. Chem.* **1972**, *11*, 2227.

(23) (a) The structure of $[Au_2\{\mu\text{-}(CH_2)_2PPh_2\}(\mu\text{-}S_2CNEt_2)]$[23b] also has been established by X-ray crystallography. Two molecules are bonded through an intermolecular gold−gold interaction, thus forming a linear chain (the maximum deviation from the linearity is 6.5°) of four gold atoms with Au−Au(intramolecular) 2.867, 2.868 Å and Au−Au (intermolecular) 2.984 Å. (b) Bardaji, M.; Connelly, N. G.; Gimeno, M. C.; Jimenez, J.; Jones, P. G.; Laguna, M.; Laguna, A. *J. Chem. Soc., Dalton Trans.* **1994**, 1163. (c) Li, D.; Che, C. M.; Peng, S. M.; Liu, S. T.; Zhou, Z. Y.; Mak, T. C. W. *J. Chem. Soc., Dalton Trans.* **1993**, 189.

(24) Uson, R.; Laguna, M.; Laguna, A.; Jimenez, J.; Jones, P. G. *Angew. Chem., Int. Ed. Engl.* **1991**, *30*, 198.

(25) Schmidbaur, H.; Graf, W.; Muller, G. *Angew. Chem., Int. Ed. Engl.* **1988**, *27*, 417.

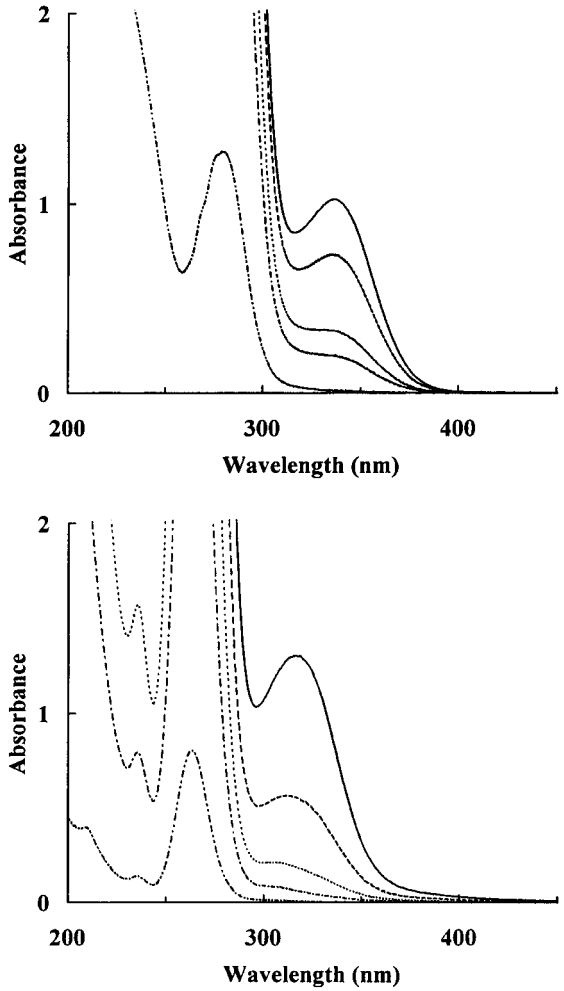

Figure 5. (a) Top: Concentration-dependent absorption spectra of **1** in acetonitrile at 298 K. Key: 7.6×10^{-3} M (—), 5.7×10^{-3} M (- - -), 3.8×10^{-3} M (···), 2.8×10^{-3} M (- · -), 4.5×10^{-4} M (- · · -). (b) Bottom: Concentration-dependent absorption spectra of **5** in acetonitrile at 298 K. Key: 1.8×10^{-2} M (—), 9.8×10^{-3} M (- - -), 4.7×10^{-3} M (···), 2.2×10^{-3} M (- · -), 2.8×10^{-4} M (- · · -). Path length = 0.1 cm.

digold unit LAu--AuL (L = phosphine) and molecular hydrogen[26] on the reaction level.

A search of the Cambridge Structural Database (CSD) for the common molecular connectivity of Au−PCH_2P−Au has resulted in 40 reliable X-ray structures with R < 10% and a total of 64 fragments (as Supporting Information). Among these structures, the Au−Au distances range from 2.755 to 3.711 Å (the second largest is 3.341 Å). Out of a total 64 fragments, there are 50 with the P−Au--Au−P torsional angle less than 20°. The mean of 64 torsional angles is 13.130°. It seems to suggest that a dppm backbone is able to bring the two Au centers into close proximity for a favorable Au−Au attraction as is evidenced statistically by the low torsional angles of P−Au--Au−P. The tendency of P−Au--Au−P toward being planar is enhanced if more than one cyclic link is present to connect the two Au centers; for example, $Au_2(dppm)Cl_2$ has an angle of 2.8° and the digold dimer cation **1** has an angle of 11.1°.

On the other hand, a CSD search for the connectivity of Au−PCH_2CH_2P−Au has resulted in 16 reliable X-ray structures with R < 10% (as Supporting Information). Among the 21 occurrences, the majority totaling 12 with 2.9 Å < Au−Au < 6.3 Å exhibit a *gauche* conformation of P−Au--Au−P (the torsional angles range from 26.5 to 72.4°). The large range of Au−Au distances is indicative of less Au−Au interaction. Only two fragments with Au−Au of ca. 2.82 Å in length and as part of a metal cluster show a cis conformation of P−Au--Au−P. The rest are 4 fragments with Au−Au > 6.8 Å in addition to a trans P−C−C−P linkage and, hence, are probably not relevant in the above discussion on the conformation of P−Au--Au−P. If each crystallographically observed conformation is regarded as a sample point of the molecular potential energy surface, the minimum energy geometry for Au−PCH_2CH_2P−Au is statistically the *gauche* conformation along the Au−Au axis, different from the *cis* conformation for Au−PCH_2P−Au.

Electronic Absorption and Emission Studies. Electronic absorption studies were used to illustrate the occurrence of molecular association of **1** and **5** in solution. The absorption spectrum of **1** (Figure 5a) in acetonitrile at room temperature shows a shoulder at about 230 nm, a band at 280 nm, and a low-energy band at about 340 nm. The absorption spectra are concentration dependent. The band at 340 nm grows faster than expected from Beer's law with increasing concentration. Some time ago, Gray *et al.* reported that $[Rh(CNPh)_4]^+$ dimerizes in solution and gives a concentration-dependent electronic absorption spectrum,[27] in which the band assigned to the formation of the dimer originating from a Rh_2 metal centered (MC) transition grows with increasing concentration. Recently, concentration-dependent UV−vis spectra of $Au(PPhMe_2)I$ were reported as evidence of molecular association.[28] Again, the growing band was assigned to a MC transition involving Au_2. If we assume that the monomer **1** is in equilibrium with the dimer of **1** (eq 1), eq 2 can be

$$2[Au_2(dppm)[(CH_2)_2S(O)NMe_2]BF_4 \rightleftharpoons [Au_2(dppm)[(CH_2)_2S(O)NMe_2]]_2(BF_4)_2 \quad (1)$$

$$[Au]_0/A_2^{1/2} = 1/(\epsilon_2 Kb)^{1/2} + 2A_2^{1/2}/\epsilon_2 b \quad (2)$$

derived, where $[Au]_0$ is the initial concentration of the monomer, A_2 is the absorbance of the dimer at 340 nm, ϵ_2 is the absorptivity coefficient of the dimer, b is the cell path length, and K is the equilibrium constant. A plot of $[Au]_0/A_2^{1/2}$ vs $A_2^{1/2}$ gives a straight line suggesting that the assumption is correct. From the slope of this plot the absorptivity coefficient (ϵ_2) of 9842 M^{-1} cm^{-1} for the dimer is obtained, and from the intercept an equilibrium constant (K) of 33 ± 9 M^{-1} is obtained. The analysis strongly suggests that the 340 nm absorption originates from a Au_4 ^{1}MC transition of the dimer. Compound **5** was also examined in detail in acetonitrile solution. The dimer of this complex absorbs at 320 nm (Figure 5b). A plot of $[Au]_0/A_2^{1/2}$ vs $A_2^{1/2}$ for this band is again a straight line whose slope and intercept yield

(26) Bruce, M. I.; Corbin, P. E.; Humphrey, P. A.; Koutsantounis, G. A.; Liddell, M. J.; Tiekink, E. R. T. *J. Chem. Soc., Chem. Commun.* **1990**, 674.

(27) (a) Mann, K. R.; Gordon, J. G.; Gray, H. B. *J. Am. Chem. Soc.* **1975**, *97*, 3553. (b) Mann, K. R.; Lewis, N. S.; Williams, R. M.; Gray, H. B.; Gorden, J. G. *Inorg. Chem.* **1978**, *17*, 828.

(28) Toronto, D. V.; Weissbart, B.; Tinti, D. S.; Balch, A. L. *Inorg. Chem.* **1996**, *35*, 2484.

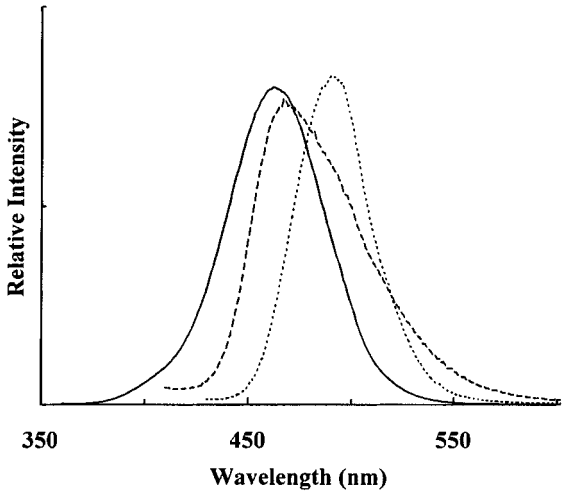

Figure 6. Solid-state emission spectra of **1** (···), **4** (—), and **5** (- - -) at 298 K.

$\epsilon_2 = 2900\ M^{-1}\ cm^{-1}$ and $K = 52 \pm 7\ M^{-1}$. The favored association constant for **5** is likely due to the sterically less crowded dmpm ligand, since up to the concentration of 10^{-2} M the absorption spectrum of **4** shows no additional band below 300 nm. The possibility of the formation of the dimer of **4** is negligible consistent with the crystal structure of **4**. In a separate work, we have also observed that electronic absorption spectra of annular $[Au_2(diphosphine)(dithiolate)](PF_6)$ are concentration dependent.[29] There the growing band at ~350 nm is assigned to a MC transition from a dimer and the monomer−dimer equilibrium constants (38 and 137 M^{-1}) are similar to the values found in this work.

Excitation of solid samples of **1**, **4**, and **5** at room temperature at $\lambda \sim 360$ nm produces intense luminescences at $\lambda_{max} = 493$, 463, and 473 nm, respectively. The solid-state emission spectra of **1**, **4**, and **5** are shown in Figure 6. These emissions have relatively long luminescent lifetime (>2 μs) and are structureless. Possible sources of the emission observed in this work are originating from (1) intraligand (IL) transitions involving the phenyl ring of phosphine or sulfur ylide ligands, (2) charge transfer (CT) transitions, and (3) metal-centered (MC) transitions. Although metal-perturbed IL transitions from phenyl rings of phosphine have been reported to occur at such similar transition energies,[30] this possibility is the least likely in this system, because **5** does not have phenyl rings. Furthermore a solid sample of the sulfoximine salt does not luminesce at room temperature under UV light. Therefore CT and MC transitions are the two most likely sources of emission. MC transitions have been assigned to gold(I) compounds having a P−Au−C moiety.[31] Transition energies between 19 531 and 23 474 cm^{-1} were observed. Although similar transition energies (~21 000 cm^{-1}) have been observed for compounds **1**, **4**, and **5**, these energies are higher than the majority of those reported values (~18 000 cm^{-1}) assigned to MC transitions.[10a,d,e,11] We therefore prefer to assign the emissive nature of our compounds as CT transitions. The order of emission energies of these three compounds is **1** < **5** < **4**. This order can be interpreted by assigning the nature of emission to a ligand to metal charge transfer transition with the excitation from an orbital primarily associated with gold to the phosphorus-based orbital. The difference in the transition energy between **1** and **4** is due to the difference in the number of gold−gold interactions. Red shifts of CT (S → Au) excitation in the presence of Au−Au interactions have been observed for gold phosphine thiolate compounds.[32] Similar argument can be applied to the Au → P CT excitation. Au−Au interaction destabilizes the filled Au(5d) antibonding orbital and thereby decreases the Au → P excitation transition energy. Crystal structure results reveal that compound **1** has three short Au−Au contacts while **4** has only one. The more the number of Au−Au interactions the compound has, the more the transition energy is decreased. The smaller transition energy found in **1** compared to that of **4** is therefore justified. Compounds **1** and **5** in acetonitrile have the same order of equilibrium constant; therefore, they may have the same number of molecular associations in the solid state. The slight difference in the emission energies (858 cm^{-1}) is likely due to the difference of electronic effects in the phosphine substituents. The methyl substituents in **5** are more electron donating than the phenyl groups in **1**. A blue shift is expected for a MLCT transition from a compound with the dppm ligand compared to the dmpm ligand. Therefore the emission energy of **5** shifts blue with respect to that of **1**.

Summary

We have demonstrated that the application of the PTC technique leads to the successful synthesis of the gold(I) sulfur-ylide complexes. Compounds **1**−**3** are synthesized by tuning different stoichiometric amounts of reactants. The PTC technique also promotes the dppm deprotonation reaction. Deprotonation of a coordinated dppm ligand is facile and reversible. The deprotonated dppm promotes ylide complex formation such that higher yields of **1** and **2** are obtained. When sterically allowed, gold(I) sulfur-ylide compounds tend to aggregate. Thus in the solid state, two cations of **1** are packed together such that four Au atoms are in a row with the intermolecular Au−Au distance shorter than intramolecular Au−Au distance. The preference of Au−Au interactions leads to the formation of tetranuclear compounds **2** and **3**. The former has one of the ylidic carbon atoms bridging two gold(I) atoms in the structure. **1** and **5** also tend to dimerize in acetonitrile as evidenced by the concentration-dependent electronic absorption spectra. The existence of unsupported Au−Au interactions in solution implies the uniqueness of gold chemistry. The equilibrium constants, *K*, between the monomer and dimer are found to be 33 and 52 M^{-1}, respectively. **1** and **5** in the solid state have long-lived emissions with high intensity under visible light. The physical and chemical properties and the potential usefulness of this type of compound deserve further study.

(29) Submitted for publication.
(30) (a) Kunkely, H.; Vogler, A. *Chem. Phys. Lett.* **1989**, *164*, 621. (b) Segers, D. P.; DeArmond, M. K.; Grutsch, P. A.; Kutal, C. *Inorg. Chem.* **1984**, *23*, 2874.
(31) Yam, V. W. W.; Choi, W. K. *J. Chem. Soc., Dalton Trans.* **1994**, 2057.
(32) Forward, J. M.; Bohmann, D.; Fackler, J. P., Jr.; Staples, R. J. *Inorg. Chem.* **1995**, *34*, 6330.

Table 1. Crystal Data and Refinement Details for Compounds 1−4

	1	2	3	4
formula	$C_{29}H_{32}Au_2NOP_2SBF_4$	$C_{54}H_{52}Au_4NOP_4SBF_4 \cdot H_2O$	$C_{50}H_{40}Au_4Cl_3P_4 \cdot C_2H_6O$	$C_{30}H_{34}Au_2NOP_2SPF_6 \cdot 2CH_2Cl_2$
fw	985.31	1779.65	1705.04	1227.33
space group	*C*2/*c*	$P\bar{1}$	$P\bar{1}$	*C*2/*c*
a, Å	22.799(3)	13.064(3)	11.773(3)	29.498(7)
b, Å	11.590(2)	13.584(3)	16.156(4)	17.192(3)
c, Å	24.662(5)	16.876(3)	17.351(6)	17.321(4)
α, deg	90	95.93(2)	109.55(2)	90
β, deg	104.80(1)	89.90(2)	98.85(2)	101.19(2)
γ, deg	90	103.47(2)	111.36(2)	90
V, Å^3	6300.4(18)	2896.0(10)	2749.5(13)	8617(3)
Z	8	2	2	8
D_c, g/cm^3	2.078	2.041	2.059	1.892
F(000)	3727.02	1667.54	1585.57	4687.01
diffractometer	CAD4	CAD4	CAD4	CAD4
X-ray radiation	Mo Kα	Mo Kα	Mo Kα	Mo Kα
μ, mm^{-1}	9.49	10.27	10.90	7.24
transm factors	0.607−0.999	0.640−1.000	0.585−0.999	0.722−0.999
no. of unique reflns	4113 ($2\theta < 45°$)	7425 ($2\theta < 45°$)	7169 ($2\theta < 45°$)	5642 ($2\theta < 45°$)
no. of obsns	2709, $I_0 > 2.5\,\sigma(I_0)$	4867, $I_0 > 2.5\sigma(I_0)$	5214, $I_0 > 2.5\sigma(I_0)$	1640, $I_0 > 2.5\sigma(I_0)$
no. of atoms	73	125	111	90
no. of params	325	826	562	492
R	0.034	0.057	0.039	0.048
R_w	0.040	0.067	0.048	0.052
GOF	1.80	2.48	2.80	1.74

Experimental Section

The ^{1}H and ^{31}P{^{1}H} NMR spectra were recorded on a Bruker AC-F300 spectrometer at 300 and 121.5 MHz, respectively. Chemical shifts, *δ*, are reported relative to the internal standard TMS for ^{1}H NMR and external standard 85% H_3PO_4 for ^{31}P NMR. Absorption spectra were obtained by a Shimadzu UV-2101PC spectrophotometer. Room-temperature emission spectra and emission lifetimes on the order of microseconds were measured on a Aminco-Bowman luminescence spectrometer. Emission lifetimes up to the nanosecond range were recorded by using an Edinburgh Analytical Instruments CD900 spectrometer. Microanalyses were performed by the Taiwan Instrumentation Center. $Au_2(dppm)Cl_2$,[33] $Au_2(dppe)Cl_2$,[33] $Au_2(dmpm)Cl_2$,[31] and $[Me_2S(O)NMe_2]]BF_4$[34] were prepared by the reported methods.

$[Au_2(dppm)((CH_2)_2S(O)NMe_2)]BF_4$, 1. Method a. $Au_2(dppm)Cl_2$ (0.59 g, 0.70 mmol) and $[Me_2S(O)NMe_2]BF_4$ (0.73 g, 3.50 mmol) in CH_2Cl_2 (10 mL) was combined with *n*-Bu_4NCl (0.01 g, 0.04 mmol) as the phase-transferring agent followed by NaOH addition (3 mL, 0.46 N). The resultant solution was stirred at room temperature for 8 h. The organic layer was then separated, washed with H_2O (10 mL) four times, and dried by a rotavapor under reduced pressure. The crude product (yield > 80%) was recrystallized from a $CH_3OH-CH_2Cl_2$ mixture (20:1 by volume). White crystals (compound **2**) precipitated in the early stages were filtered out (20% yield). Slow evaporation of the filtrate gives a 52% yield of greenish crystals (compound **1**).

Method b. 3 (0.015 g, 8.7×10^{-3} mmol) was treated with $[Me_2S(O)NMe_2]BF_4$ (0.01 g, 4.35×10^{-2} mmol) in CH_2Cl_2 (10 mL), and then *n*-Bu_4NCl (0.001 g, 4.35×10^{-3} mmol) was added as the phase-transferring agent followed by NaOH (0.435 mL, 0.20 N). After a similar workup as mentioned in method a, **1** can be isolated in 80% yield. Anal. Calcd for $C_{29}H_{32}BF_4NOP_2SAu_2$: C, 35.3; H, 3.3; N, 1.4. Found: C, 35.3; H, 3.2; N, 1.3. Mp: 220 °C dec. ^{31}P NMR ($CDCl_3$): 36.44 ppm. ^{1}H NMR ($CDCl_3$): 7.60 (m, 20H, C_6H_5), 3.67 (m, 2H, SCH_2), 3.41, 3.24 (t, d, 2H, $^2J_{HH} = 14$ Hz, $^2J_{HP} = 12$ Hz, PCH_2), 2.94 (s, 6H, NCH_3), 2.70 (m, 2H, SCH_2). FAB/MS: *m*/*z* 898, $(M - BF_4)^+$.

$[Au_4(dppm)(Ph_2PCHPPh_2)[(\mu\text{-}CH)(CH_2)S(O)NMe_2]]BF_4 \cdot H_2O$, 2. $[Me_2S(O)NMe_2]BF_4$ (0.003 g, 1.53×10^{-2} mmol) was combined with CH_2Cl_2 (20 mL) with *n*-Bu_4NCl (0.0004 g, 1.53×10^{-3} mmol) added as the phase-transferring agent followed by NaOH (13.9 *μ*L, 1.80 N). The resultant solution was stirred at room temperature for 1 h. Then this solution was combined with compound **3** (0.025 g, 1.53×10^{-2} mmol) and stirred at room temperature for an additional 12 h. The organic layer was then separated, washed with H_2O (20 mL) three times, and dried by a rotavapor under reduced pressure. The crude product (yield > 80%) was recrystallized from a CH_2Cl_2-EtOH (95%) mixture (1:1 by volume). White crystals were obtained. Yield: 50%. Anal. Calcd for $C_{54}H_{54}BF_4NO_2P_4SAu_4$: C, 36.5; H, 3.1; N, 0.8. Found: C, 36.6; H, 3.0; N, 0.8. ^{31}P NMR ($CDCl_3$): 36.44 (d, $^3J_{PP} = 14$ Hz), 36.33 (d, $^3J_{PP} = 14$ Hz), 32.87 (d, t, $^2J_{PP} = 52$ Hz, $^3J_{PP} = 14$ Hz), 28.00 (d, $^2J_{PP} = 52$ Hz). ^{1}H NMR ($CDCl_3$): 8.00−6.82 (m, 40H, C_6H_5), 3.90−3.50 (m, 4H, PCH_2, PCH, SCH), 3.03 (s, 6H, NCH_3), 2.54 (m, 1H, SCH), 2.34 (m, 1H, SCH). FAB/MS: *m*/*z* 1674, $[M - (BF_4 + H_2O)]^+$.

$[Au_4(dppm)(Ph_2PCHPPh_2)Cl_3]$, 3. $[Me_2S(O)NMe_2]BF_4$ (0.05 g, 0.23 mmol) was added to a solution of $Au_2(dppm)Cl_2$ (0.20 g, 0.23 mmol) in CH_2Cl_2 (50 mL) followed by the addition of *n*-Bu_4NCl (0.006 g, 0.02 mmol) and NaOH (0.567 mL, 0.20 N). The solution was stirred for 24 h at ambient temperature and then washed with water and dried by rotavapor under a reduced pressure. Crystalline materials can be obtained from recrystallization in an acetone/EtOH/CH_2Cl_2 mixed solvent (1:1:1 ratio by volume). Yield: 70%. **3** also can be produced under the same conditions without the sulfoxonium salts, but the yield is low. Anal. Calcd for $C_{50}H_{43}P_4Cl_3Au_4$: C, 35.9; H, 2.6. Found: C, 36.1; H, 2.6. ^{31}P NMR ($CDCl_3$): 35.53 (d, t, $^2J_{PP} = 63$ Hz, $^3J_{PP} = 15$ Hz), 30.36 (d, $^3J_{PP} = 15$ Hz), 24.73 (d, $^2J_{PP} = 63$ Hz). ^{1}H NMR ($CDCl_3$): 8.42−7.00 (m, 40H, C_6H_5, 4.60 (t, d, 1H, $^2J_{HP} = 12$ Hz, $^3J_{HP} = 7$ Hz), 3.35 (t, 2H, $^2J_{HP} = 12$ Hz).

$[Au_2(dppe)[(CH_2)_2S(O)NMe_2]]PF_6$, 4. $Au_2(dppe)Cl_2$ (0.32 g, 0.37 mmol) and $[Me_2S(O)NMe_2]]BF_4$ (0.39 g, 1.85 mmol) were dissolved in CH_2Cl_2 (30 mL). To this solution was added *n*-Bu_4NCl (0.006 g, 0.02 mmol) followed by NaOH (18 mL, 0.20 N). The resultant solution was stirred at room temperature for 8 h. The organic layer was separated, washed with water four times, and then reduced to 5 mL. To this organic solution, 5 drops of NH_4PF_6 saturated in EtOH was added. The white precipitate thus formed was filtered out and recrystallized from CH_2Cl_2/hexane. The yield of the colorless crystalline material was 60%. Anal. Calcd for $C_{30}H_{34}F_6NOP_3SAu_2$: C, 34.1; H, 3.2; N, 1.3. Found: C, 33.3; H, 3.2; N, 1.3. Mp: 150 °C dec. ^{31}P NMR ($CDCl_3$): 35.79 ppm. ^{1}H NMR ($CDCl_3$): 7.76−7.49 (m, 20H, C_6H_5), 3.52 (m, 2H, SCH_2), 2.92 (s, 6H,

(33) Schmidbaur, H.; Wohlleben, A.; Wagner, F.; Orama, O.; Huttner, G. *Chem. Ber.* **1977**, *110*, 1748.
(34) Johnson, C. R.; Rogers, P. E. *J. Org. Chem.* **1973**, *38*, 1793.

NCH_3), 2.80 (d, 4H, $^2J_{HP}$ = 12 Hz, PCH_2), 2.67 (m, 2H, SCH_2). FAB/MS: *m*/*z* 912, $(M - PF_6)^+$.

Compound **5** was synthesized in an analogous way as that described for compound **4**. Characterization data are given below.

$[Au_2(dmpm)[(CH_2)_2S(O)NMe_2]]BF_4$, 5. The yellowish microcrystals were obtained by recrystallization from CH_2Cl_2/hexane. Anal. Calcd for $C_9H_{24}F_4BNOP_2SAu_2$: C, 14.7; H, 3.3; N, 1.9. Found: C, 14.6; H, 3.3; N, 2.0. Mp: 182 °C dec. ^{31}P NMR ($CDCl_3$): 15.97 ppm. ^1H NMR ($CDCl_3$): 3.08 (m, 2H, SCH_2), 2.88 (s, 6H, NCH_3), 2.71, 2.40 (t, d, 2H, $^2J_{HH}$ = 13 Hz, $^2J_{HP}$ = 15 Hz, PCH_2), 2.54 (m, 2H, SCH_2), 1.80 (m, 12H, $^{2+4}J_{HP}$ = 10 Hz, PCH_3). FAB/MS: *m*/*z* 650, $(M - BF_4)^+$.

X-ray Structure Analyses. The single-crystal X-ray diffraction measurements were performed on a Nonius CAD-4 automated diffractometer using graphite-monochromated Mo Kα radiation. A total of 25 high-angle reflections were used in a least-squares fit to obtain accurate cell constants. Diffraction intensities were collected up to $2\theta < 45°$ using the $\theta/2\theta$ scan technique, with background counts made for half the total scan time on each side of the peak. Three standard reflections, measured every 1 h, showed no significant decay in intensity during data collection. The reflections with $I_0 > 2.0\sigma(I_0)$ or $2.5\sigma(I_0)$ were judged as observations and were used for solution and structure refinement. Data were corrected for Lorentz−polarization factors. An empirical absorption correction based on a series of ψ scans was applied to the data. The structure was solved by direct methods[35] and refined by a full-matrix least-squares routine[36] with anisotropic thermal parameters for all non-hydrogen atoms (weight = $1/[\sigma(F_o)^2 + 0.0001(F_o)^2]$, $\sigma(F_o)$ from counting statistics). All the hydrogen atoms were placed isotropically at their calculated positions (C−H = 1.00 Å) and fixed in the calculations. Atomic scattering factors were taken from ref 37. For a summary of crystal data and refinement details, see Table 1. Selected bond distances and angles are given in the figure captions.

Acknowledgment. We thank the National Science Council of Taiwan (ROC; Grant Nos. NSC 84−2113-M-031-002 and NSC 85-2113-M-031-009) for financial support.

Supporting Information Available: Tables giving data collection parameters, positional and isotropic thermal parameters, anisotropic thermal parameters, and bond lengths and angles for all of the structural analyses and data from the Cambridge Structure Database (42 pages). Ordering information is given on any current masthead page.

OM960748J

(35) Main, P. In *Crystallographic Computing 3: Data Collection, Structure Determination, Proteins and database*; Sheldrick, G. M., Krueger, C., Goddard, R., Eds.; Clarendon Press: Oxford, U.K., 1985; p 206.

(36) Gabe, E. J.; Le Page, Y.; White, P. S.; Lee, F. L. *Acta Crystallogr.* **1987**, *43A*, S294.

(37) *International Tables for X-ray Crystallography*; Ibers, J. A., Hamilton, W. C., Eds.; Kynoch: Birmingham, U.K., 1974.